PHYSICAL REVIEW D VOLUME 49, NUMBER 7 1 APRIL 1994

Transverse momentum distributions for heavy quark pairs

Edmond L. Berger
High Energy Physics Division, Argonne National Laboratory, Argonne, Illinois 60439
and CERN, Geneva, Switzerland

Ruibin Meng*
High Energy Physics Division, Argonne National Laboratory, Argonne, Illinois 60439
(Received 26 October 1993)

We study the transverse momentum distribution for a *pair* of heavy quarks produced in hadron-hadron interactions. Predictions for the large transverse momentum region are based on exact order α_s^3 QCD perturbation theory. For the small transverse momentum region, we use techniques for all orders resummation of leading logarithmic contributions associated with initial state soft gluon radiation. The combination provides the transverse momentum distribution of heavy quark pairs for all transverse momenta. Explicit results are presented for $b\bar{b}$ pair production at the Fermilab Tevatron collider and for $c\bar{c}$ pair production at fixed target energies.

PACS number(s): 13.85.Ni, 12.38.Bx

I. INTRODUCTION

The distribution in the transverse momentum $q_\perp$ of a heavy quark *pair* $Q\bar{Q}$ produced in hadron-hadron interactions is of interest for elucidating the underlying quantum chromodynamics (QCD), and its understanding is important in studies of B-$\bar{B}$ mixing and CP violation at hadronic facilities. Unlike the case of pairs of heavy quarks produced in e^+e^- annihilation, $Q\bar{Q}$ pairs created in hadron-hadron collisions are often not in a back-to-back configuration (even in a plane transverse to the beam direction). The net transverse momentum of the pair measures the imbalance between the transverse momenta of the $\bar{Q}$ and the Q. In this paper, we examine the quantitative description in QCD perturbation theory of the expected imbalance. Predictions for the region of large $q_\perp$ are based on exact order α_s^3 QCD perturbation theory. For the regions of small and modest $q_\perp$, we employ an all orders resummation of leading logarithmic contributions associated with the emission of soft gluons from the intial-state partons that participate in the hard scattering process. This calculation addresses a practical question for heavy quark tagging at hadron facilities: If a Q is tagged with a given transverse momentum, what distribution in transverse momentum should one expect to observe for the associated $\bar{Q}$?

We consider the process hadron+hadron $\to Q+\bar{Q}+X$. In the simplest parton model description, the underlying hard scattering process is parton + parton $\to Q+\bar{Q}$. At this level of approximation, no bremsstrahlung gluons are radiated from initial-state or final-state partons. If one neglects intrinsic transverse momentum of initial-state partons, $q_\perp$ is zero. Therefore, in the simplest parton model description, Q and $\bar{Q}$ pairs would be produced back to back in the transverse plane. However, gluon bremsstrahlung is important in QCD and in general generates nonzero $q_\perp$.

The single particle inclusive differential cross section for heavy quark production has been studied in detail at next-to-leading order in QCD. We cite in particular the calculation of the complete first order corrections to the dominant QCD production channels [1, 2] and [3–5] and comparisons with data on inclusive b-quark production from the UA1 [6] and Collider Detector at Fermilab (CDF) Collaborations [7]. We mention also the recent work on resummation of leading logarithmic contributions for the one particle inclusive cross section [8]. In the single particle inclusive approach, the kinematical variables of the heavy quark's (or antiquark's) partner and of the final-state light partons are integrated over with the attendant limitation that it is not possible to examine quark-antiquark correlations or the cross section differential in the transverse momentum q_T of the $Q\bar{Q}$ pair. Correlations have been studied at leading order [9] and at next-to-leading order [10, 11]. One may expect that next-to-leading order QCD should provide reliable expectations for the distribution in q_T at large q_T. At small q_T, the relatively large mass m_Q of the heavy quark Q justifies perturbation theory, but the presence of the two disparate scales m_Q and q_T requires care.

Perturbative QCD has been used for a successful description of transverse momentum distributions in massive lepton-pair production, the Drell-Yan process [12]. There one studies the reaction hadron + hadron $\to e^+ + e^- + X$, where the electron-positron pair is detected and its transverse momentum $q_\perp$ is measured [13–16]. Important for the quantitative description of the transverse momentum distribution at modest values of $q_\perp$ is the resummation of logarithmic contributions associated with emission of soft gluons in the initial state of the hard scattering process quark + antiquark $\to e^+ + e^- + X$. We follow closely the analogy with the Drell-Yan case for the reaction hadron + hadron $\to Q + \bar{Q} + X$ and concentrate on the transverse momentum distribution of the $Q\bar{Q}$ quark pair. Heavy quark pair production is, however, more involved than massive lepton-pair production.

*Present address: Department of Physics and Astronomy, University of Kansas, Lawrence, KS 66045.

New complications arise from soft gluon emission from the final-state heavy quarks, effects that are absent in the Drell-Yan reaction. We will argue that the resummation technique for dealing with initial gluon radiation should still be applicable in our case. Soft gluon emission from final-state heavy quarks has been studied in [17].

For the process hadron + hadron $\rightarrow Q + \bar{Q} + X$, we choose to study the cross section differential in the variables M^2 and $q_\perp^2$; M is the invariant mass of the $Q\bar{Q}$ pair. Knowing M and $q_\perp$, we can judge how far the $Q\bar{Q}$ system is away from the back-to-back configuration in the transverse plane. To be more specific, when M is near the mass threshold $2m$ of the $Q\bar{Q}$ pair, the momenta of the Q and $\bar{Q}$ are close to zero in the center of mass frame of the $Q\bar{Q}$ system. Only a small amount of $q_\perp$ then suffices to put the Q and $\bar{Q}$ in a configuration that is not back to back in the transverse plane in the laboratory system of reference. On the other hand, at large M, the Q and $\bar{Q}$ have large relative momentum in the center of mass frame of the pair. At large M, large $q_\perp$ would be needed to produce a $Q\bar{Q}$ pair that is not back to back in the transverse plane in the laboratory system.

At large and moderate values of $q_\perp^2 = O(M^2)$, the $Q\bar{Q}$ pair production cross section can be computed perturbatively as

$$\frac{d\sigma}{dM^2 dq_\perp^2} = \alpha_s^3(a_1 + a_2\alpha_s + a_3\alpha_s^2 + \cdots). \tag{1}$$

At any fixed order of α_s and $q_\perp^2 \neq 0$, the cross section is well behaved after the hard scattering cross section has been properly defined. At low $q_\perp^2 \neq 0$, however, the convergence of the perturbative series deteriorates. For small $q_\perp^2 \neq 0$, the dominant contributions (i.e., the leading logarithmic contributions) to Eq. (1) have the form

$$\frac{d\sigma}{dM^2 dq_\perp^2} \sim \frac{\alpha_s^2}{q_\perp^2}\left[b_1\alpha_s \ln\left(\frac{M^2}{q_\perp^2}\right) + b_2\alpha_s^2 \ln^3\left(\frac{M^2}{q_\perp^2}\right) + \cdots\right]. \tag{2}$$

The convergence of the theory is therefore governed by $\alpha_s \ln^2(M^2/q_\perp^2)$ instead of α_s. The logarithms arise through emission of soft and collinear gluons. At sufficiently low $q_\perp^2$, $\alpha_s \ln^2(M^2/q_\perp^2)$ is large even when α_s is small and any fixed order calculation breaks down. In order to obtain a reliable prediction, one must resum the leading contributions to all orders in α_s.

The remainder of this paper is organized as follows. In Sec. II we present the perturbative calculation of the $q_\perp^2$ distribution using exact order α_s^3 QCD matrix elements. We describe how to obtain the asymptotic expression at $q_\perp^2 \rightarrow 0$ from the exact order α_s^3 matrix elements. In Sec. III we discuss the formalism for resumming the initial soft and collinear gluon contributions. We match the resummed result in the low-$q_\perp^2$ region to the exact $\mathcal{O}(\alpha_s^3)$ result in the high-$q_\perp^2$ region. Results and examples of the $q_\perp^2$ distribution for specific hadronic reactions are given in Sec. IV.

II. PERTURBATIVE CALCULATION

We begin our discussion with the hadronic reaction in which a $Q\bar{Q}$ pair is produced:

$$p(K_1) + \bar{p}(K_2) \rightarrow Q(p_1) + \bar{Q}(p_2) + X. \tag{3}$$

In this expression, p and $\bar{p}$ denote the proton and antiproton, respectively. The quantity X stands for all the final particle states that we sum over so that the above process is semi-inclusive with respect to the outgoing final particles. We use capital letters for the momenta of the proton and antiproton to distinguish them from those of the quarks, antiquarks, and gluons. The corresponding partonic subprocess can be written as

$$p_i(k_1) + p_j(k_2) \rightarrow Q(p_1) + \bar{Q}(p_2) + X, \tag{4}$$

where $p_{i,j}$ are the initial partons from the proton and the antiproton. The relationship between the momenta of the hadrons and partons is

$$k_1 = \xi_1 K_1, \quad k_2 = \xi_2 K_2. \tag{5}$$

The four-momentum of the system made up of the $Q\bar{Q}$ pair is

$$q^\mu = p_1^\mu + p_2^\mu. \tag{6}$$

We also define several useful invariants for our calculation:

$$\begin{aligned} S &= (K_1 + K_2)^2, \\ s &= (k_1 + k_2)^2 = \xi_1\xi_2 S, \\ M^2 &= q^2 = (p_1 + p_2)^2, \\ x_1 &= \frac{M^2}{2q\cdot K_1}, \quad x_2 = \frac{M^2}{2q\cdot K_2}, \\ Y &= \frac{1}{2}\ln(q\cdot K_2/q\cdot K_1) \equiv y + \frac{1}{2}\ln(\xi_1/\xi_2), \\ q_\perp^2 &= \frac{2q\cdot K_1\, q\cdot K_2}{K_1\cdot K_2} - M^2 = \frac{2q\cdot k_1\, q\cdot k_2}{k_1\cdot k_2} - M^2. \end{aligned} \tag{7}$$

We remark that $\sqrt{S}$ is the collision energy of the proton and antiproton; M is the invariant mass of the heavy quark $Q\bar{Q}$ pair; $q_\perp^2$ is the square of the transverse momentum of the pair, equal to the square of the vector sum of the individual transverse momenta of the Q and $\bar{Q}$; Y is the rapidity of the $Q\bar{Q}$ pair in the center of mass frame of the proton and antiproton; and y is the rapidity of the $Q\bar{Q}$ pair in the center of mass frame of the interacting initial partons.

The differential cross section for reaction (3) is expressed as a convolution of partonic cross sections and parton distribution functions:

$$\frac{d^2\sigma_{p\bar{p}\rightarrow Q\bar{Q}X}}{dM^2 dq_\perp^2 dY} = \sum_{i,j=q,\bar{q},g}\int_{\tau_{\min}}^1 d\xi_1 \int_{\tau_{\min}/\xi_1}^1 d\xi_2\; f_{i/p}(\xi_1,\mu)\, f_{j/\bar{p}}(\xi_2,\mu)\frac{d^2\hat{\sigma}_{ij\rightarrow Q\bar{Q}X}}{dM^2 dq_\perp^2 dy}. \tag{8}$$

Here $\tau_{\min} = (\sqrt{M^2+q_\perp^2}+q_\perp)^2/S$, and $d^2\hat{\sigma}_{ij\to Q\bar{Q}X}/dM^2dq_\perp^2dy$ is the fixed-order reduced partonic cross section obtained by first calculating Feynman diagrams up to a given fixed order in QCD perturbation theory and then implementing a renormalization scheme to remove any ultraviolet divergences. The soft divergences at $q_\perp \to 0$ are canceled between the virtual diagrams and the bremsstrahlung diagrams. The collinear divergences (mass singularities) at $q_\perp \to 0$ are absorbed into the definition of the parton distribution functions. Therefore the fixed-order reduced partonic cross section is well behaved for any value of $q_\perp^2$, in particular $q_\perp^2 = 0$. [Note that the apparent divergence at $q_\perp^2 = 0$ in Eq. (2) is canceled by a δ function that arises from virtual diagrams.] An advantage of calculating the order α_s^3 differential cross section in terms of $q_\perp^2$ is that $q_\perp^2$ can be used as a cutoff variable for both the infrared and collinear divergences in the bremsstrahlung diagram calculations. This means that at any finite value of $q_\perp^2$, the order α_s^3 differential cross section can be calculated by evaluating the bremsstrahlung diagrams without explicit concern about soft gluon cancellation and factorization of the collinear singularity.

We now consider $Q\bar{Q}$ pair production in QCD perturbation theory. It proceeds by the following two reactions in the Born approximation (order α_s^2):

$$q(k_1)+\bar{q}(k_2)\to Q(p_1)+\bar{Q}(p_2),$$
$$g(k_1)+g(k_2)\to Q(p_1)+\bar{Q}(p_2). \tag{9}$$

The symbols inside the parentheses denote the momentum assignments for the partons. The Feynman graphs that contribute to the Born amplitude are shown in Fig. 1.

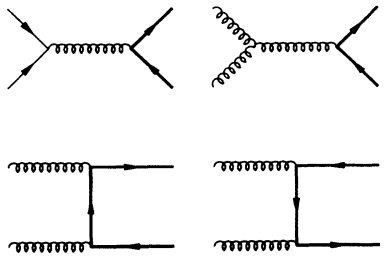

FIG. 1. Feynman diagrams at order α_s^2.

The magnitude squared of the Born amplitude, averaged over initial colors and spins and summed over final colors and spins, can be written as [18]

$$\overline{|M|}^2_{q\bar{q}\to Q\bar{Q}} = \frac{g_s^4}{N}C_F A_{\rm QED},$$
$$\overline{|M|}^2_{gg\to Q\bar{Q}} = \frac{g_s^4}{N^2-1}\left(C_F - C_A\frac{t_1u_1}{s}\right)B_{\rm QED}, \tag{10}$$

with

$$A_{\rm QED} = \frac{t_1^2+u_1^2}{s}+\frac{2m^2}{s},$$
$$B_{\rm QED} = \frac{t_1}{u_1}+\frac{u_1}{t_1}+\frac{4m^2s}{t_1u_1}\left(1-\frac{m^2s}{t_1u_1}\right); \tag{11}$$

t_1 and u_1 are defined as

$$t_1 = (k_2-p_2)^2-m^2, \quad u_1 = (k_1-p_2)^2-m^2. \tag{12}$$

It is easy to verify that

$$\frac{d\sigma^{(0)}_{q\bar{q},gg\to Q\bar{Q}}}{dM^2dq_\perp^2dy} = \delta\left(1-\frac{x_1}{\xi_1}\right)\delta\left(1-\frac{x_2}{\xi_2}\right)\delta(q_\perp^2)\frac{\sigma^{(0)}_{q\bar{q},gg}(M^2)}{M^2}. \tag{13}$$

The total partonic cross sections are [19]

$$\sigma^{(0)}_{q\bar{q}}(M^2) = \frac{2\pi\alpha_s^2}{3M^2}\frac{C_F}{N}\beta(1+2m^2/M^2), \tag{14}$$

$$\sigma^{(0)}_{gg}(M^2) = \frac{2\pi\alpha_s^2}{M^2}\frac{C_F}{N^2-1}\left[-\left(1+\frac{4m^2}{M^2}\right)\beta-\left(1+4\frac{m^2}{M^2}-\frac{8m^4}{M^4}\right)\ln x\right]$$
$$+\frac{2\pi\alpha_s^2}{M^2}\frac{C_A}{N^2-1}\left[\left(-\frac{1}{3}-\frac{5}{3}\frac{m^2}{M^2}\right)\beta-\frac{4m^4}{M^4}\ln x\right], \tag{15}$$

with

$$\beta = \sqrt{1-4m^2/M^2}, \quad x = \frac{1-\beta}{1+\beta}. \tag{16}$$

The C_A and C_F are the Casimir invariants for the adjoint and the fundamental representation of SU(N). For the particular case of SU(3),

$$N=3, \quad C_A = N, \quad C_F = \frac{N^2-1}{2N}. \tag{17}$$

Observe that the differential cross section Eq. (13) is proportional to $\delta(q_\perp^2)$, because in the Born approximation the heavy quark pairs are produced with $q_\perp^2 = 0$. The total partonic cross sections $\sigma^{(0)}_{q\bar{q}}(M^2)$ and $\sigma^{(0)}_{gg}(M^2)$ are inversely proportional to M^2. This dependence can be understood because the lowest order graphs either have only s-channel poles or fermion exchange lines. Most of the heavy quark pairs are therefore expected to be produced near threshold, $M^2 = 4m^2$.

At order α_s^3 the contributing partonic subprocesses include gluon bremsstrahlung diagrams and (anti)quark-gluon scattering diagrams:

$$q(k_1)+\bar{q}(k_2)\to g(k_3)+Q(p_1)+\bar{Q}(p_2),$$
$$g(k_1)+g(k_2)\to g(k_3)+Q(p_1)+\bar{Q}(p_2), \qquad (18)$$
$$g(k_1)+q(\bar{q})(k_2)\to q(\bar{q})(k_3)+Q(p_1)+\bar{Q}(p_2),$$

plus virtual correction diagrams [20] to the lowest order processes Eq. (9). In Fig. 2 we show some examples of the gluon bremsstrahlung diagrams that contribute at order α_s^3.

In the order α_s^3 processes (18), $q_\perp^2$ is no longer constrained to be zero; a spectrum of values of $q_\perp^2$ will be produced. The $q_\perp^2 \to 0$ limit means that the parton with momentum k_3 in the processes (18) is either soft and/or collinear to one of the initial- or final-state partons. We note that in the $q\bar{q}$ channel there are diagrams with a gluon emitted from an initial quark or antiquark line; these look diagrammatically exactly the same as corresponding graphs in the Drell-Yan reaction. In addition there are diagrams with a gluon emitted from a final heavy quark or antiquark line; these are absent in the Drell-Yan reaction. The initial gluon emission diagrams can be soft and/or collinear divergent at $q_\perp^2 \to 0$. The final gluon emission diagrams can have only a soft divergence at $q_\perp^2 \to 0$ because the final-state quarks are massive. The same statements can be made for the gluon-gluon-initiated subprocesses which are usually the dominant processes for $Q\bar{Q}$ pair production. The quark-gluon scattering diagrams have only a collinear divergence from light quark emission. The square of the matrix element for the order α_s^3 processes Eq. (18) has been published [21]. We will make use of those results in our calculation.

To calculate the partonic differential cross section $d\sigma^{(1)}_{ij\to Q\bar{Q}k}/dM^2dq_\perp^2dy$ at order α_s^3 we must integrate over variables which are independent of M^2, $q_\perp^2$, and y for the

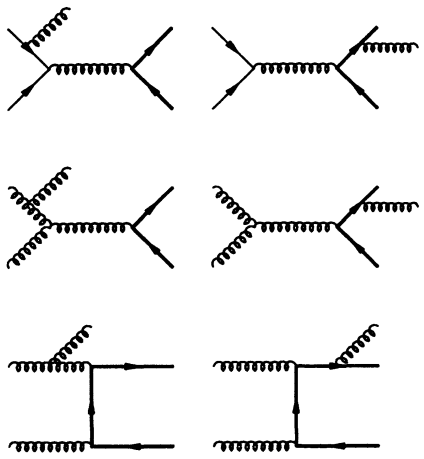

FIG. 2. Examples of order α_s^3 Feynman diagrams with a gluon emitted from an initial quark or gluon line or from final heavy quark line.

gluon bremsstrahlung and quark-gluon scattering processes. We choose the $Q\bar{Q}$ center of mass frame in which

$$q^\mu=(p_1+p_2)^\mu = (M,\ 0,\ 0,\ 0),$$
$$p_1^\mu=(M/2,\ \omega_0\sin\theta_1\sin\theta_2,\ \omega_0\sin\theta_1\cos\theta_2,\ \omega_0\cos\theta_1),$$
$$p_2^\mu=(M/2,\ -\omega_0\sin\theta_1\sin\theta_2,\ -\omega_0\sin\theta_1\cos\theta_2,\ -\omega_0\cos\theta_1), \qquad (19)$$

with

$$\omega_0=\frac{M}{2}\sqrt{1-4m^2/M^2}. \qquad (20)$$

We obtain

$$\frac{d\sigma^{(1)}_{ij\to Q\bar{Q}k}}{dM^2dq_\perp^2dy}(\text{pert})=\frac{1}{128\pi^4 sM^2}\frac{x_1}{\xi_1}\frac{x_2}{\xi_2}\,\delta\left(\left(1-\frac{x_1}{\xi_1}\right)\left(1-\frac{x_2}{\xi_2}\right)-\frac{q_\perp^2/M^2}{1+q_\perp^2/M^2}\right)$$
$$\times\int\frac{d^3p_1}{2p_1^0}\,\delta((q-p_1)^2-m^2)\,\overline{|M|}^2_{ij\to Q\bar{Q}k}. \qquad (21)$$

The integral $\int d^3p_1$ can be expressed explicitly as

$$\int\frac{d^3p_1}{2p_1^0}\,\delta((q-p_1)^2-m^2)\,\overline{|M|}^2_{ij\to Q\bar{Q}k}=\frac{1}{8}\sqrt{1-4m^2/M^2}\int_0^\pi d\theta_1\sin\theta_1\int_0^{2\pi}d\theta_2\,\overline{|M|}^2_{ij\to Q\bar{Q}k}, \qquad (22)$$

and $\overline{|M|}^2_{ij\to Q\bar{Q}k}$ is the square of the matrix element for the order α_s^3 processes (18), averaged over spin and color.

It is possible to perform the angular integrations analytically. However, the squared matrix elements for the $Q\bar{Q}$ production process are lengthy and the integrals are difficult, making the calculation formidable. Fortunately, for any finite value of $q_\perp^2$ the order α_s^3 differential cross section Eq. (21) is free from any soft and collinear divergences so that the angular integrals Eq. (22) can be dealt with numerically. Then the differential cross section for the proton antiproton reaction, Eq. (3), can be calculated by convoluting the partonic cross section Eq. (21) with the parton distribution functions according to Eq. (8).

A quantity of interest and importance is the average of the square of the transverse momentum at a fixed invariant mass M. It can be calculated as [22]

$$\langle q_\perp^2(M)\rangle\left(\frac{d\sigma_{p\bar{p}\to Q\bar{Q}X}}{dM^2}\right)=\int dq_\perp^2\,q_\perp^2\,\frac{d^2\sigma_{p\bar{p}\to Q\bar{Q}X}}{dM^2dq_\perp^2}$$
$$=\sum_{i,j=q,\bar{q},g}\int_{M^2/S}^1 d\xi_1\int_{M^2/(\xi_1 S)}^1 d\xi_2\,f_{i/p}(\xi_1,\mu)\,f_{j/\bar{p}}(\xi_2,\mu)\int_0^{(s-M^2)^2/(4s)}dq_\perp^2\,q_\perp^2\,\frac{d^2\sigma^{(1)}_{ij\to Q\bar{Q}k}}{dM^2dq_\perp^2}, \qquad (23)$$

where

$$\frac{d\sigma_{p\bar{p}\to Q\bar{Q}X}}{dM^2} = \sum_{i,j=q,\bar{q},g}\int_{M^2/S}^1 d\xi_1 \int_{M^2/(\xi_1 S)}^1 d\xi_2\; f_{i/p}(\xi_1,\mu)\, f_{j/\bar{p}}(\xi_2,\mu)\left[\frac{d\hat{\sigma}^{(0)}_{ij\to Q\bar{Q}}}{dM^2} + \frac{d\hat{\sigma}^{(1)}_{ij\to Q\bar{Q}X}}{dM^2}\right]$$

$$\equiv \mathcal{K}\sum_{i,j=q,\bar{q},g}\int_{M^2/S}^1 d\xi_1 \int_{M^2/(\xi_1 S)}^1 d\xi_2\; f_{i/p}(\xi_1,\mu)\, f_{j/\bar{p}}(\xi_2,\mu)\frac{d\hat{\sigma}^{(0)}_{ij\to Q\bar{Q}}}{dM^2}. \tag{24}$$

$\mathcal{K}$ denotes the familiar K factor, not necessarily a constant in this case. The transverse momentum averaged over all values of invariant mass can also be calculated in the same way.

As remarked in the Introduction, the convergence of the perturbation series deteriorates in the region $q_\perp^2 \ll M^2$. For predictions of improved reliability in that domain, one must try to sum leading contributions from all orders in α_s. We will use the procedure for resumming contributions from initial-state soft and collinear gluons developed by Collins and Soper [13]. To begin, we must first extract the leading contributions in the region of small $q_\perp^2 \ll M^2$ from the α_s^3 cross section. This is done by calculating the angular integrals in Eq. (22) analytically. Fortunately, in the limit $q_\perp^2/M^2 \to 0$ the squared matrix element simplifies substantially and the angular integrals can be calculated analytically without too much difficulty [3].

We take the limit $q_\perp^2 \to 0$ of the exact expressions for the square of the order α_s^3 matrix elements and do the integration under the same limit. The calculation is accomplished in two steps. First, we calculate the soft gluon contributions by setting the gluon momentum $k_3 \to 0$ everywhere in the matrix elements except in the denominators that are singular as $k_3 \to 0$. The soft gluon matrix elements have also been derived in the literature [see Eqs. (5.1–5) in Ref. [3] and Eqs. (2.24–26) in Ref. [4]]. In the limit $k_3 \to 0$, the $2 \to 3$ kinematics can also be approximated by $2 \to 2$ kinematics, which we can implement effectively by replacing the δ function in Eq. (21) by

$$\delta\left(\left(1-\frac{x_1}{\xi_1}\right)\left(1-\frac{x_2}{\xi_2}\right) - \frac{q_\perp^2/M^2}{1+q_\perp^2/M^2}\right)$$

$$\Longrightarrow \ln\left(\frac{M^2}{q_\perp^2}\right)\delta\left(1-\frac{x_1}{\xi_1}\right)\delta\left(1-\frac{x_2}{\xi_2}\right). \tag{25}$$

The singularities in the denominator can be replaced by

$$\left(1-\frac{x_1}{\xi_1}\right)\left(1-\frac{x_2}{\xi_2}\right) \Longrightarrow \frac{q_\perp^2}{M^2}. \tag{26}$$

Second, the hard collinear contributions can be calculated if we replace the first δ function in Eq. (21) by

$$\delta\left(\left(1-\frac{x_1}{\xi_1}\right)\left(1-\frac{x_2}{\xi_2}\right) - \frac{q_\perp^2}{1+q_\perp^2/Q^2}\right)$$

$$\Longrightarrow \frac{\delta(1-x_1/\xi_1)}{(1-x_2/\xi_2)_+} + \frac{\delta(1-x_2/\xi_2)}{(1-x_1/\xi_1)_+}. \tag{27}$$

The + prescription in the above equation, defined as

$$\int_0^1 \frac{f(x)}{(1-x)_+}dx = \int_0^1 \frac{f(x)-f(1)}{1-x}dx, \tag{28}$$

ensures that there is no double counting in the phase space region where the soft and collinear divergences overlap. Both replacements Eq. (25) and Eq. (27) imply significant simplification for our calculation. Their origin has been well demonstrated, e.g., in Eqs.(2.11–13) of Ref. [23]. After we perform the angular integrations and convolution with the parton distribution functions we obtain the asymptotic expression for the differential cross section for process (3) in the form

$$\frac{d^3\sigma_{p\bar{p}\to Q\bar{Q}X}}{dM^2\, dq_\perp^2\, dY}(\text{asym}) = \sum_{i,j=q,\bar{q},g}\sigma_{ij}^{(0)}(M^2)\,\frac{1}{S}\,\frac{\alpha_s(M^2)}{2\pi}\,\frac{1}{q_\perp^2}\left\{\left[\mathcal{A}_{ij}^{(1)}\ln\left(\frac{M^2}{q_\perp^2}\right) + \mathcal{B}_{ij}^{(1)}\right] f_{i/p}(x_1) f_{j/\bar{p}}(x_2)\right.$$

$$\left. + \Big[f_{i/p}(x_1)\Big(P_{j\leftarrow b}\otimes f_{b/\bar{p}}\Big)(x_2) + \Big(P_{i\leftarrow a}\otimes f_{a/p}\Big)(x_1) f_{j/\bar{p}}(x_2)\Big]\right\}. \tag{29}$$

The symbol $\otimes$ denotes a convolution of the parton distribution function f and Altarelli-Parisi splitting function P, defined by

$$\Big(f\otimes P\Big)(x) \equiv \int_x^1 f(y)\, P\left(\frac{x}{y}\right)\frac{dy}{y}. \tag{30}$$

The functions $\mathcal{A}_{ij}^{(1)}$ come purely from initial-state soft and collinear gluon radiation:

$$\mathcal{A}_{q\bar{q}}^{(1)} = 2C_F, \quad \mathcal{A}_{gg}^{(1)} = 2C_A, \quad \mathcal{A}_{q(\bar{q})g}^{(1)} = 0. \tag{31}$$

The functions $\mathcal{B}_{ij}^{(1)}$ can be split into two parts, in terms of initial- and final-state gluon radiation:

$$\mathcal{B}_{ij}^{(1)} = B_{ij,I}^{(1)} + B_{ij,F}^{(1)}, \tag{32}$$

with

$$B^{(1)}_{q\bar{q},I} = -3C_F, \quad B^{(1)}_{q\bar{q},F} = 2C_F + 2C_F\frac{\ln x}{\beta}(1-2m^2/M^2),$$
$$B^{(1)}_{gg,I} = -2\beta_0, \quad B^{(1)}_{gg,F} = 2C_F + 2C_F\frac{\ln x}{\beta}(1-2m^2/M^2), \tag{33}$$
$$B^{(1)}_{q(\bar{q})g,I} = 0, \quad B^{(1)}_{q(\bar{q})g,F} = 0.$$

Quantities x and β have been defined in Eq. (16). Our coefficient β_0 of the β function is normalized to

$$\beta_0 = \frac{11N - 2N_f}{6}. \tag{34}$$

To verify our calculation we have checked that the $1/\epsilon^2$, $1/\epsilon$ pole terms generated by dimensional regularization from the terms not proportional to the Altarelli-Parisi splitting functions in the expression Eq. (29) cancel the infrared pole terms from virtual diagram calculations [3, 4].

The expressions for the initial-state gluon radiation terms for the $q\bar{q}$ channel, $\mathcal{A}^{(1)}_{q\bar{q}}$ and $B^{(1)}_{q\bar{q},I}$, are exactly the same as those in the Drell-Yan reaction. For initial-state gluon radiation in the gg channel, our expressions $\mathcal{A}^{(1)}_{gg}$ and $B^{(1)}_{gg}$ also agree with those found by Catani, D'Emilio, and Trentadue [25] and by Kauffman [23] for production of a color singlet state from gluon-gluon fusion. The agreement in both cases follows the expectation that the initial-state soft gluon radiation does not depend on the type of hard process under consideration [26, 27]. It indicates that the effects of initial-state gluon radiation can be resummed to all orders of α_s for $Q\bar{Q}$ pair production, as in the cases of the Drell-Yan reaction [13, 14] or Higgs boson production through gluon fusion [24, 25, 23]. In the next section we will attempt the resummation of the initial soft and collinear gluon contributions using the formalism developed for the Drell-Yan process [28, 29].

The expressions for final-state soft gluon radiation, $B^{(1)}_{q\bar{q},F}$ and $B^{(1)}_{gg,F}$, are the same for the $q\bar{q}$ and gg channels. This can be understood since the final-state soft gluon radiation occurs from the final-state (anti)heavy quark lines in both the $q\bar{q}$ and gg channels. Soft gluon emission from final-state heavy quarks has been studied in Ref. [17].

III. RESUMMATION

The technique for resumming contributions from initial-state soft and collinear gluons was developed by Collins and Soper [29], and it has been applied to massive lepton-pair production [14], single vector boson production [30, 31], Higgs boson production [24, 25, 23, 32], and ZZ-pair production [33]. In our case, the appropriate expression analogous to that of Collins and Soper is

$$\frac{d^3\sigma}{dM^2\,dq_\perp^2\,dY}(\text{resum}) = \sum_{i,j=q,\bar{q},g} \sigma^{(0)}_{ij}(M^2)\,\frac{1}{2S}\int_0^\infty db\,b\,J_0(b\,q_\perp)\,W_{ij}(M,b)\,, \tag{35}$$

where $J_0(x)$ is the zeroth order Bessel function. The function $W_{ij}(M,b)$ sums all the logarithmic terms of the form $\alpha_s^n \ln^m(M^2b^2)$ with $1 \le m \le 2n$ in the impact parameter b space. The all orders structure of W is given by the functional form

$$W_{ij}(M,b) = \exp\left\{-\int_{C_1^2/b^2}^{C_2^2M^2}\frac{dq^2}{q^2}\left[\ln\left(\frac{C_2^2M^2}{q^2}\right)A_{ij}(\alpha_s(q^2)) + B_{ij}(\alpha_s(q^2))\right]\right\}$$
$$\times\left(C\otimes f_{i/p}\right)\left(x_1,\frac{C_3^2}{b^2}\right)\left(C\otimes f_{j/\bar{p}}\right)\left(x_2,\frac{C_3^2}{b^2}\right). \tag{36}$$

The parameters C_1, C_2, and C_3 are somewhat arbitrary. They are associated with the choices of renormalization and factorization scales in a fixed-order perturbative calculation. We use the standard choices

$$C_1 = C_3 = 2e^{-\gamma_E} = b_0, \quad C_2 = 1, \tag{37}$$

where γ_E is Euler's constant. The symbol $\otimes$ denotes a convolution, defined in Eq. (30). In the limit $q_\perp/M \to 0$, the parton momentum fractions are

$$x_1 = e^Y\sqrt{\frac{M^2}{S}}\,, \quad x_2 = e^{-Y}\sqrt{\frac{M^2}{S}}\,. \tag{38}$$

The functions A, B, and $C(x)$ may be expanded in a perturbation series in α_s:

$$A_{ij}(\alpha_s) = \sum_{n=1}^\infty A_{ij}^{(n)}\left(\frac{\alpha_s}{2\pi}\right)^n,$$
$$B_{ij}(\alpha_s) = \sum_{n=1}^\infty B_{ij}^{(n)}\left(\frac{\alpha_s}{2\pi}\right)^n, \tag{39}$$
$$C_{ij}(x,\alpha_s) = \delta_{i\bar{j}}\,\delta(1-x) + \sum_{n=1}^\infty C_{ij}^{(n)}\left(\frac{\alpha_s}{2\pi}\right)^n.$$

The reason for the bar over the j in the expression for $C_{ij}(x,\alpha_s)$ is that the flavors of i and j must be the same in the case of $q\bar{q}$.

We work to first order in the expansions of A and B which corresponds to summing the first two powers of $\ln(M^2/q_\perp^2)$ at every order in α_s, i.e, the double-leading

logarithm approximation. The $A_{ij}^{(n)}$'s and $B_{ij}^{(n)}$'s depend implicitly on the choices of $C_{1,2,3}$. The simplest forms result from the choices in Eq. (37). The coefficients $A_{ij}^{(1)}$ and $B_{ij}^{(1)}$ in Eq. (39) can be obtained by formally expanding Eq. (35) in a series in α_s and then comparing with the asymptotic perturbative calculation from our previous section. For initial-state gluon radiation, the expressions for $A_{ij}^{(1)}$ in Eq. (39) are the $\mathcal{A}_{ij}^{(1)}$ of Eq. (31), and the $B_{ij}^{(1)}$ are the $B_{ij,I}^{(1)}$ in Eq. (33). For C, we make the simplifying choice $C_{ij}^{(0)} = \delta_{i\bar{j}}\,\delta(1-x)$ since we are working in perturbation theory to the first nontrivial order in α_s for large $q_\perp$. [Note that $\sigma_{ij}^{(0)}$ in Eq. (35) is proportional to α_s^2.] Our neglect of $C_{ij}^{(1)}$ will only affect the normalization at $q_\perp = 0$ to $O(\alpha_s^3)$ and the distribution for $q_\perp \neq 0$ to $O(\alpha_s^4)$. These statements imply that our calculation includes resummation of the double-leading logarithms to all orders in α_s, but the total integrated cross section is accurate only to second order in α_s.

We comment that the validity of the resummation formalism [29] was demonstrated for the Drell-Yan reaction and for W, Z production where there is no final-state gluon radiation. We are making the reasonable assumption here that the same formalism is valid for dealing with the effects of initial-state soft and collinear gluon radiation in the case of heavy quark pair production. Resummation of soft gluon emission from the final-state heavy quarks has been studied in Ref. [17].

The gluon resummation formula, Eq. (35), provides the cross section in the region of small $q_\perp$; for the high-$q_\perp$ region we use the exact $O(\alpha_s^3)$ perturbative calculation. We will join the results for the low-$q_\perp$ and high-$q_\perp$ regions using a matching procedure employed previously [24, 23]:

$$\frac{d\sigma}{dM^2\,dq_\perp^2\,dy}\,(\text{match}) = \frac{d\sigma}{dM^2\,dq_\perp^2\,dy}\,(\text{pert}) + f(q_\perp/M)\left[\frac{d\sigma}{dM^2\,dq_\perp^2\,dy}\,(\text{resum}) - \frac{d\sigma}{dM^2\,dq_\perp^2\,dy}\,(\text{asym})\right]. \tag{40}$$

The function

$$f(q_\perp/M) = \frac{1}{1+(3q_\perp/M)^4} \tag{41}$$

serves to switch smoothly from the matched formula to the perturbative formula [23]. For details of the matching procedure we refer the reader to papers by Arnold and Kauffman [31] and subsequent publications.

Before presenting numerical evaluations, we end this section with a few remarks. As discussed by Parisi and Petronzio [28], the resummed expression Eq. (36) is ill defined when $b \geq 1/\Lambda_{\rm QCD}$ because confinement sets in and α_s diverges. Procedures have been proposed in the literature [28, 29, 14] to deal with this difficulty and parametrize nonperturbative effects. In this paper we follow the method used by Collins and Soper [29] and by Davies and collaborators [14]. We replace $W(b)$ in Eq. (36) by

$$W(b) \to W(b_*)e^{-S_{\rm NP}(b)}, \tag{42}$$

$$b_* = \frac{b}{\sqrt{1+b^2/b_{\rm max}^2}}. \tag{43}$$

Large values of b are thereby cut off at some $b_{\rm max}$; $\exp[-S_{\rm NP}(b)]$ parametrizes the large-b dependence due to nonperturbative physics. In principle, $\exp[-S_{\rm NP}(b)]$ can be measured, but in practice one can approximate the function with a simple Gaussian parametrization:

$$S_{\rm NP}(b) = b^2[g_1 + g_2\ln(b_{\rm max}M/2)]. \tag{44}$$

According to Davies and collaborators [14],

$$g_1 = 0.15\ \text{GeV}^2,\quad g_2 = 0.4\ \text{GeV}^2,\quad b_{\rm max} = (2\text{GeV})^{-1}. \tag{45}$$

The values of g_1 and g_2 are obtained by fitting massive lepton-pair production data at $\sqrt{S} = 27$ and 62 GeV. There is no strong reason to believe that the contribution from nonperturbative intrinsic transverse momentum should be identical for subprocesses initiated by gluon-gluon scattering, as in our case, and quark-antiquark scattering, as in massive lepton-pair production. When substantial samples of data become available on $c\bar{c}$ and $b\bar{b}$ production, it should be possible to refine the choices made here. Particularly informative in this respect will be data on the azimuthal angle (ϕ) dependence. The extent to which the quark and antiquark are produced with ϕ near π is particularly sensitive to the net transverse momentum imparted to the quark-antiquark pair [10, 11].

IV. RESULTS AND DISCUSSION

In this section we present and discuss some phenomenological applications of our analysis. We use Harriman-Martin-Roberts-Stirling (HMRS) parton distribution functions [34] and the one-loop-corrected formula for the running coupling constant $\alpha_s(\mu)$ with $\Lambda_4 = 190$ MeV. The factorization scale and the renormalization scale are chosen to be the same as the invariant mass of the heavy quark $Q\bar{Q}$ pair, i.e., $\mu = M$, unless stated otherwise.

In Fig. 3 we show the lowest order result for the distribution in invariant mass of a $b\bar{b}$ pair produced in a $p\bar{p}$ collision at the Fermilab collider energy $\sqrt{S} = 1.8$ TeV. The bottom quark mass is chosen as $m_b = 4.75$ GeV. The distribution peaks at a value of M a few GeV above the $b\bar{b}$ pair mass threshold of $2m_b$. It then decreases quickly as M increases. This implies that most b's and/or $\bar{b}$'s are produced at the Fermilab collider with small momentum in the $b\bar{b}$ center of mass frame. Next-to-leading order QCD contributions change the overall normalization of this curve, but more important for the sake of our present discussion, they should not change the shape of the low-

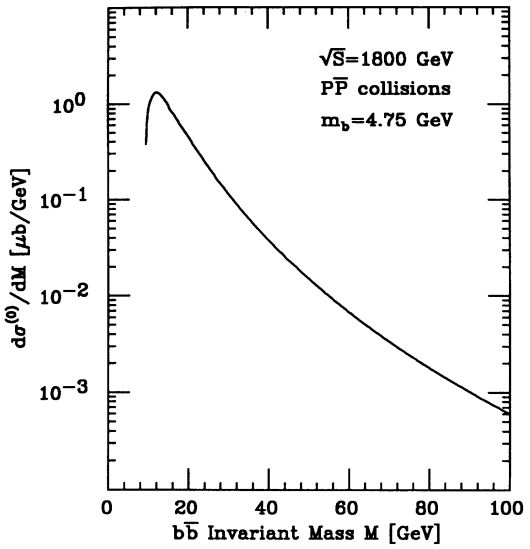

FIG. 3. $b\bar{b}$ pair invariant mass distribution computed from lowest order QCD processes.

est order curve except very near threshold or far above threshold [35].

In Fig. 4, the average quantity $\langle q_\perp^2(M)\rangle\mathcal{K}$ is plotted as a function of the pair invariant mass M; the factor $\mathcal{K}$ was discussed in Sec. II. The quantity $\langle q_\perp^2(M)\rangle\mathcal{K}$ is proportional to the square of the average transverse momentum of the $b\bar{b}$ pair. Its value is about 80 GeV^2 near threshold and rises linearly with M in the range shown in the figure. At the fixed rapidity value $Y = 0$, the function has the same shape and magnitude as in Fig. 4, understandable because the $b\bar{b}$ pairs are produced centrally. (An approximately linear rise with M of the average transverse

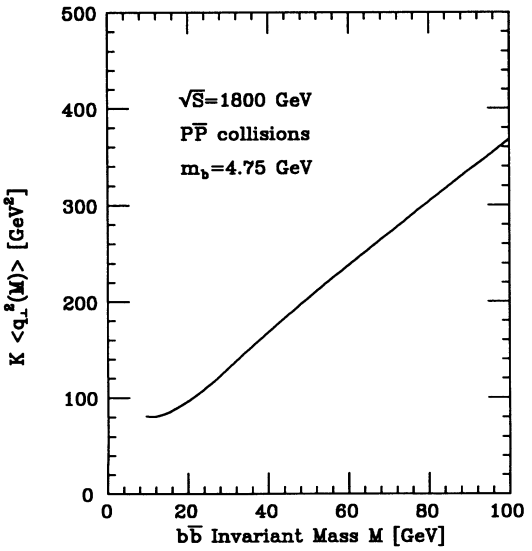

FIG. 4. Average of the square of the transverse momentum of a $b\bar{b}$ pair, multiplied by the factor K, as a function of the pair invariant mass M. This curve is obtained from the purely perturbative order α_s^3 calculation.

momentum in the region $\tau = M^2/S \ll 0.05$ would be expected from simple dimensional arguments. The growth of the square in Fig. 4 is less rapid than quadratic.)

An important inference may be drawn from Figs. 3 and 4. We may estimate from Fig. 3 that the average invariant mass $\langle M\rangle = 15$ GeV. Glancing at Fig. 4 we notice that near and above the pair mass threshold $\langle q_\perp^2(M)\rangle\mathcal{K}$ is larger than 80 GeV^2. Using $\mathcal{K} \sim 2.4$ (see Refs. [1, 4]), we deduce that $b\bar{b}$ pairs produced at the Fermilab collider are expected to have an average transverse momentum about 5 GeV. As will be discussed below, after integrating over all values of M, we find that the square of the average transverse momentum $\langle q_\perp^2\rangle$ is 36.0 GeV^2 in the purely perturbative order α_s^3 approximation. Taking the square root, we deduce $\langle q_\perp\rangle_{\rm rms} \sim 6$ GeV. This value is comparable to, and slightly larger than, the typical momentum of an individual b or $\bar{b}$ in the $b\bar{b}$ center of mass frame. Correspondingly, a significant fraction (about one-quarter to one-half depending upon how one defines the back-to-back configuration) of $b\bar{b}$ pairs at the Fermilab collider is expected to be produced in a configuration that is not back to back in the transverse plane.

The differential cross section $d\sigma/dMdq_\perp$ is presented in Fig. 5 for three fixed values of mass, $M = 15$, 25, and 50 GeV. The dashed curves are from our fixed-order α_s^3 perturbative calculation. They are most applicable in the region $q_\perp = O(M)$ where there is essentially only one hard scale in the problem. The fixed-order α_s^3 results become inapplicable if $q_\perp << O(M)$ where, as discussed earlier, the effects of soft gluon contributions must be incorporated in order to obtain a more reliable result. The dot-dashed lines show the asymptotic results, Eq. (29), obtained from the fixed-order α_s^3 results in the limit $q_\perp \to 0$. At small $q_\perp$ the asymptotic results agree with the perturbative results, as expected. At larger $q_\perp$, the asymptotic results manifest unphysical characteristics that can be traced to the fact that the functions $\mathcal{A}_{ij}^{(1)}$ and $\mathcal{B}_{ij}^{(1)}$ have opposite signs [cf. Eqs. (31) and (33)]. Accordingly, we take the asymptotic results at face value only at small $q_\perp$. The cross sections obtained from resummation of the effects of initial soft gluon radiation are shown by the dotted lines.

The resummed results are not expected to follow the asymptotic results because only the initial-state soft gluon radiation is included in our resummed formalism. The resummed and the purely perturbative order α_s^3 curves nearly coincide for $q_\perp$ about 5 GeV and greater, as might be expected since the mass of the bottom quark is the relevant physical scale at small $q_\perp$. Owing to the effects of resummation, the shapes of the two curves differ significantly for $q_\perp$ less than 5 GeV.

The solid lines in Fig. 5 present our final matched results, obtained from Eq. (40). The matched results agree with the resummed results in the region of small $q_\perp$ and with the perturbative results at large $q_\perp$. These three figures demonstrate how the final resummed and matched results differ from the perturbative results in the small-$q_\perp$ region. They also show that the simple matching procedure seems to work adequately in our case [36].

To preclude confusion, we stress that $d\sigma/dMdq_\perp$ is presented in Fig. 5; thus, the vanishing of the resummed

curves as $q_\perp$ goes to zero has a kinematic origin. The divergence apparent in Eq. (2) is not present in the resummed calculation.

In Fig. 6(a), the perturbative, asymptotic, and the resummed results from Fig. 5(a) are replotted as $d\sigma/dM\,dq_\perp^2$ vs $q_\perp^2$. This figure illustrates the behavior of the cross section at small $q_\perp$ in a different way, without the phase space factor of $q_\perp$ that is present in $d\sigma/dM\,dq_\perp$ shown in Fig. 5(a). The same results are plotted again in Fig. 6(b) but with the switching function Eq. (41) included as a multiplicative factor in the asymptotic and resummed results. A comparison of Figs. 6(a) and 6(b) demonstrates the effects of the switching function included in the matching formula Eq. (40). At small $q_\perp$, the switching function is close to 1 and does not modify the asymptotic and resummed results. At large $q_\perp^2 \sim 50\ \mathrm{GeV}^2$, the switching function suppresses the asymptotic and resummed results by almost a factor of 10.

In Fig. 7 our final results are shown for the distribution in the square of the transverse momentum of the $b\bar{b}$ pair, $d\sigma/dq_\perp^2$. Here we have integrated over M. As remarked at the start of this section, for consistency, all curves, including the purely perturbative order α_s^3 curve (dashed line), are computed with the one-loop-evolved form for α_s.

For $q_\perp \neq 0$, the differences between the matched (solid curve) and fixed-order α_s^3 (dashed) results in Fig. 7 are formally of order α_s^4 and higher [except that our integrated cross section is valid only to $O(\alpha_s^2)$, as explained in Sec. II]. These differences will affect, among other observables, the predicted average transverse momentum of

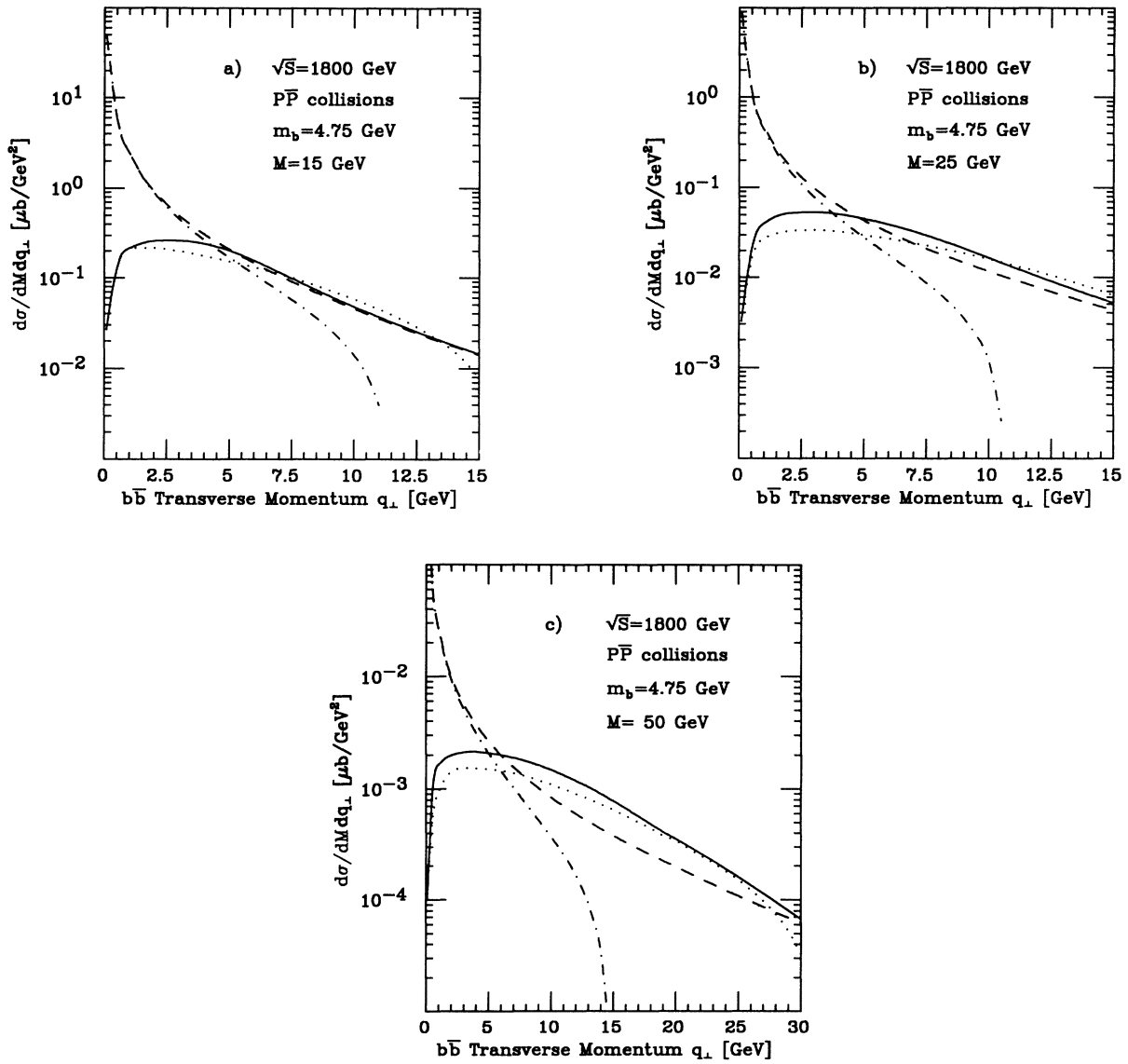

FIG. 5. $b\bar{b}$ pair transverse momentum distributions for three values of invariant mass, $M = 15$, 25, and 50 GeV. We show our fixed-order α_s^3 perturbative results as dashed lines, and our initial-state soft gluon resummed results as dotted lines. The asymptotic results are represented as dot-dashed lines. The final matched results are shown as solid lines.

the $b\bar{b}$ pair. Computations of the integrals over all $q_\perp$ of the product of $q_\perp^2$ times $d\sigma/dq_\perp^2$ are straightforward for both the solid and dashed curves in Fig. 7 since this product is finite and well behaved as $q_\perp$ approaches zero in both cases. The integral of $d\sigma/dq_\perp^2$ itself is straightforward for the matched case, where there is no divergence as $q_\perp$ approaches zero, but is more involved in the purely α_s^3 case. In the α_s^3 case, full account must be taken of virtual diagrams that contribute at $q_\perp^2 = 0$ [19, 1, 3, 4]. Carrying out the computations, we obtain $\langle q_\perp^2 \rangle = 36.0\ \mathrm{GeV}^2$ in the purely perturbative order α_s^3 approximation and $\langle q_\perp^2 \rangle = 66.7\ \mathrm{GeV}^2$ for our matched case. We have checked that use of the two-loop-evolved form for α_s changes the purely perturbative order α_s^3 value of $\langle q_\perp^2 \rangle$ by less than $1\ \mathrm{GeV}^2$.

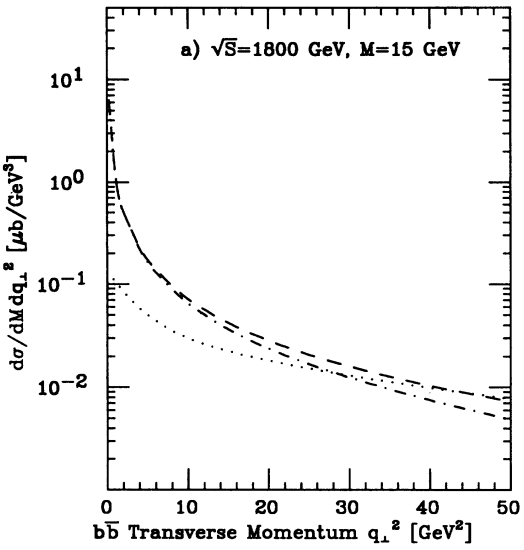

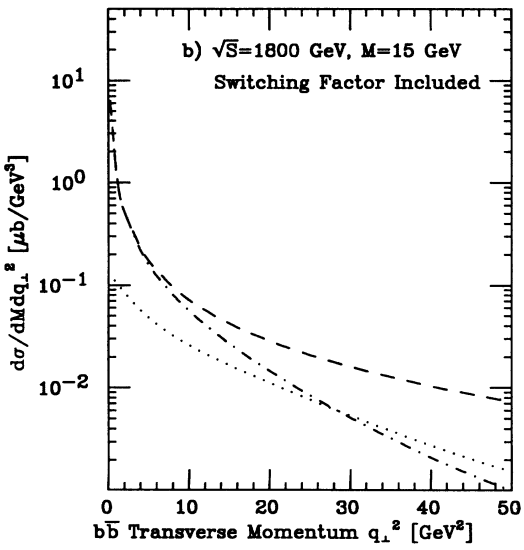

FIG. 6. (a) The perturbative, asymptotic, and resummed results from Fig. 5(a) are plotted as $d\sigma/dM\,dq_\perp^2$ vs $q_\perp^2$. (b) The same results are plotted again but with the switching function Eq. (41) included as a multiplicative factor in the asymptotic and resummed results.

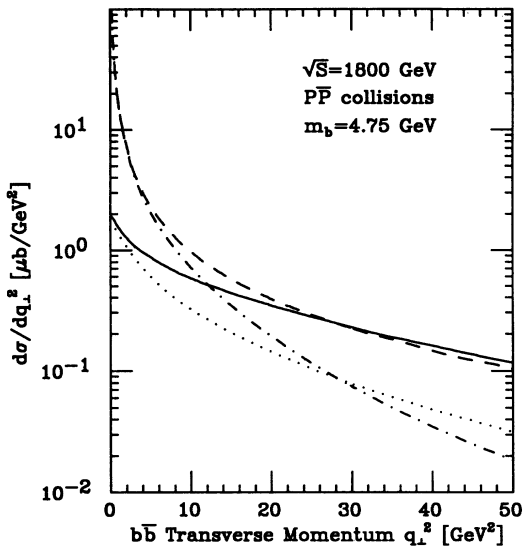

FIG. 7. Distribution in the square of the $b\bar{b}$ pair transverse momentum. Our final matched results are shown by the solid line. For small $q_\perp^2$ we integrate the leading logarithmic resummed result, Eq. (35), over M. The pure $O(\alpha_s^3)$ result is represented as the dashed curve, the initial-state soft gluon resummed result as a dotted line, and the asymptotic result as a dot-dashed line.

Using the numbers in the paragraph above, we note that $\langle q_\perp^2 \rangle$ is increased by $30.7\ \mathrm{GeV}^2$ as a result of soft gluon resummation and matching. Taking square roots, we find $\langle q_\perp \rangle_{\mathrm{rms}} \sim 8.2$ GeV in the matched case, to be compared to ~ 6 GeV in the purely perturbative order α_s^3 case. It may seem remarkable that an additional ~ 2 GeV is associated with soft gluon resummation. It would be useful to be able to compare this predicted increase with that expected for $\langle q_\perp^2 \rangle$ in massive lepton pair production (the Drell-Yan process) at Fermilab Tevatron energies, at massive lepton pair masses in the vicinity of 10–20 GeV, comparable to those for $b\bar{b}$ pair production. However, to our knowledge, no calculations have been published for the resummed $q_\perp$ distribution for the Drell-Yan process at such masses at Tevatron energies. Calculations at lower energies [29, 14] and/or higher masses [30, 31] may not be a useful guide since the distribution should broaden with energy at fixed mass. We remark, however, that the $q_\perp$ distribution should be significantly broader for $b\bar{b}$ pair production because the coefficients in the resummation expression, Eq. (36), are much larger: $\mathcal{A}_{gg}^{(1)} = 2C_A$ vs $\mathcal{A}_{q\bar{q}}^{(1)} = 2C_F$.

It would be interesting to compare the solid line in Fig. 7 with data. We comment that our result is for production of a pair of b and $\bar{b}$ quarks, not a pair of B and $\bar{B}$ mesons. To compare with measurements of the transverse momentum of a pair of B and $\bar{B}$ mesons, one must include effects associated with fragmentation of the b and $\bar{b}$ quarks, and try to estimate effects associated with final-state gluon radiation. In a Monte Carlo simulation of the single b or $\bar{b}$ inclusive spectrum, Kuebel

and collaborators showed that the effects of final-state and initial-state gluon radiation tended to compensate in some instances, with final-state radiation tending to soften the spectrum and initial-state radiation broadening the distribution [10]. To obtain the b-quark inclusive cross section, the UA1 Collaboration [6] and the CDF Collaboration [37] use a Monte Carlo procedure to take into account the fragmentation effects of b quarks into observed B mesons or single leptons before they compared their data with theoretical predictions. A similar procedure is required before comparison can be made of data with our theoretical prediction of the pair transverse momentum distribution.

In Fig. 8, we show a distribution in the square of the transverse momentum for production of a pair of charm quarks, $c\bar{c}$ pair production in a fixed-target proton beam experiment with $E_{\rm beam} = 800$ GeV. In the case of charm, the average transverse momentum is so small that nonperturbative physics may dominate in the region of small $q_\perp$. We will not dwell here on applications of the resummation method to charm pair production. In another paper, we plan to present further phenomenological applications for $b\bar{b}$ pair production.

A fundamental issue not addressed in this paper is the extent to which the complete Collins-Soper-Sterman resummation formalism beyond the leading logarithm approximation can be taken over without alteration and used in the case of heavy quark pair production. Unlike the case of massive lepton pair production, there is soft gluon radiation in the final state. This is a nonleading logarithm effect, as indicated in Eqs. (29), (32), and (33), but it will certainly change the formalism from the massive lepton pair case if one is to be complete, resulting in a different impact parameter dependence. (Soft gluon exponentiation has not been demonstrated for a color octet final state. In further research, one could consider a decomposition of the amplitudes for gluon-gluon, quark-antiquark, and gluon-quark scattering into color singlet and color octet parts, and then proceed with the soft gluon formalism only for the color singlet piece.) In this paper, as stated in the text, we resum only the initial-state radiation. In an attempt to obtain a quantitative estimate of the difference that might arise from inclusion of the subleading final-state radiation, we recomputed the resummed result (shown as a dotted line in Fig. 5) including the full expression for the functions B, not just their initial-state contributions. The resulting change is fairly slight; the most noticeable change is an increase in the magnitude of the resummed result at its peak by about a factor of 1.5, followed by a more rapid decrease with q_T. At $M = 15$ GeV, the curves cross at $q_T = 5$ GeV. It is not possible to separate initial- and final-state radiation at large q_T. We use the purely perturbative result at large q_T, meaning that final-state radiation is included there. Both intial- and final-state gluon radiation are included in our "asymptotic" contribution. Since we resum only the initial-state radiation, it is only the nonsingular pieces of the final-state radiation that are included in our answers at moderate or small q_T.

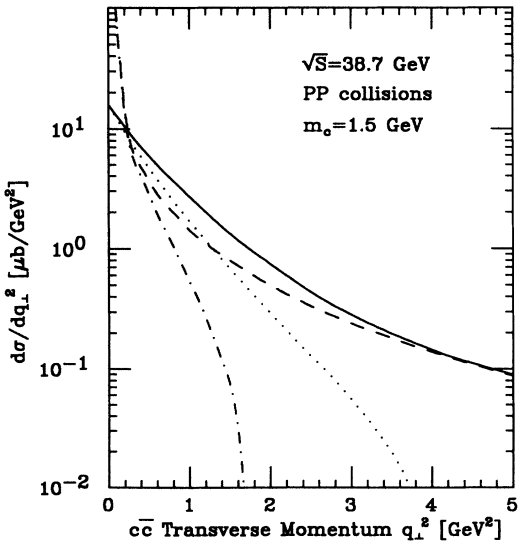

FIG. 8. Distribution in the square of the $c\bar{c}$ pair transverse momentum for proton-proton collision at $\sqrt{S} = 38.7$ GeV (corresponding to fixed-target beam energy 800 GeV). Curves are labeled as in Fig. 7.

In this paper, we have focused on the distribution in transverse momentum of a pair of heavy quarks. In carrying out our calculation, we integrated over (angular) variables in the $Q\bar{Q}$ rest frame. Correspondingly, certain limitations must be accepted. In the context of our calculation, we are not able to describe the fully differential distribution in the momenta of the Q and $\bar{Q}$ separately, notably the azimuthal angle (ϕ) dependence in the transverse plane, or correlations in rapidity. The limitation on the description of rapidity correlations appears insignificant since these differ little at leading [9] and next-to-leading order [11]. On the other hand, the azimuthal angle dependence is sensitive to the net transverse momentum imparted to the $Q\bar{Q}$ pair [11, 10], and it would be valuable to develop our approach further in order to examine the influence of soft gluon resummation on the ϕ distribution.

A calculation of the fully exclusive parton cross section for $Q\bar{Q}$ pair production at order α_s^3 has been published, along with examples of distributions at collider and fixed-target energies [11]. As in the calculation reported here, those results include the lowest order α_s^2 cross section for production of a $Q\bar{Q}$ pair, the order α_s^3 virtual corrections to the lowest order cross section, and the order α_s^3 cross section for production of a $Q\bar{Q}$ pair along with a light parton. That calculation does not include the effects of soft gluon resummation presented in this paper. On the other hand, included in Ref. [11] is an exploration of certain other effects that go beyond the pure α_s^3 QCD calculation. The parton shower Monte Carlo program HERWIG [38] was used to simulate the effects on the ϕ distribution of finite intrinsic transverse momentum of the initial partons. Substantial broadening of the ϕ distribution was observed, tantamount to what one would expect if the incident partons carried an intrinsic transverse momentum of about 1.7 GeV. While such a large intrinsic contribution was questioned in Ref. [11] as perhaps an

unreliable artifact of the parton shower algorithm, the notable influence of the added transverse momentum on the ϕ distribution underscores the importance of the type of study carried out in the present paper. We recall that our soft gluon resummation introduces substantial additional $\langle q_\perp \rangle$. As a step in the direction of a full investigation of the influence of soft gluon resummation on the ϕ distribution, it might be possible to incorporate the matched distributions shown in Figs. 7 and 8 into a modified order α_s^3 event generator.

In summary, we have studied the distribution in the transverse momentum of a pair of heavy quarks produced in hadronic reactions. For large $q_\perp$, the order α_s^3 perturbative result should be applicable. In the region of small $q_\perp$, we argued that resummation techniques developed in the study of the Drell-Yan reaction should apply for initial-state soft gluon radiation. Use of the resummation method, plus a matching of results in the small- and large-$q_\perp$ regions, permits an improved prediction of the full $q_\perp$ spectrum. Numerical results for the small-$q_\perp$ region were presented for $b\bar{b}$ pair production at the Fermilab collider and for $c\bar{c}$ pair production in fixed-target experiments.

ACKNOWLEDGMENTS

We are pleased to acknowledge useful discussions with S. Catani, J. Collins, R. Kauffman, P. Nason, W. L. van Neerven, J. Smith, B. Webber, and C-P. Yuan. This work was supported in part by the U.S. Department of Energy, Division of High Energy Physics, Contract No. W-31-109-ENG-38.

[1] P. Nason, S. Dawson, and R. K. Ellis, Nucl. Phys. **B327**, 49 (1989).

[2] G. Altarelli, M. Diemoz, G. Martinelli, and P. Nason, Nucl. Phys. **B308**, 724 (1988); E. L. Berger, in *Physics in Collison* 9, Jerusalem, 1989, edited by J. Grunhaus (Editions Frontieres, France, 1990), pp. 101–117; E. L. Berger, R. Meng, and J.-W. Qiu, in *Proceedings of the XXVI International Conference on High Energy Physics*, Dallas, Texas, 1992, edited by J. R. Sanford, AIP Conf. Proc. No. 272 (AIP, New York, 1993), Vol. 1, p. 853.

[3] W. Beenakker, H. Kuijf, W. L. van Neerven, and J. Smith, Phys. Rev. D **40**, 54 (1989).

[4] W. Beenakker, W. L. van Neerven, R. Meng, G. Schuler, and J. Smith, Nucl. Phys. **B351**, 507 (1991).

[5] R. Meng, W. L. van Neerven, G. Schuler, and J. Smith, Nucl. Phys. **B339**, 325 (1990).

[6] UA1 Collaboration, C. Albajar *et al.*, Phys. Lett. B **213**, 4105 (1988); Z. Phys. C **48**, 1 (1990); Phys. Lett. B **256**, 121 (1991).

[7] CDF Collaboration, F. Abe *et al.*, Phys. Rev. Lett. **68**, 3403 (1992); **69**, 3704 (1992); **71**, 2537 (1993); **71**, 500 (1993); **71**, 2396 (1993).

[8] E. Laenen, J. Smith, and W. L. van Neerven, Nucl. Phys. **B369**, 543 (1992).

[9] E. L. Berger, Phys. Rev. D **37**, 1810 (1988).

[10] D. Kuebel, M. Pundurs, C. P. Yuan, E. L. Berger, and F. E. Paige, Phys. Rev. D **43**, 767 (1991).

[11] M. L. Mangano, P. Nason, and G. Ridolfi, Nucl. Phys. **B373**, 295 (1992); **B405**, 507 (1993); CERN Report No. CERN-TH.6921/93 (unpublished).

[12] S. D. Drell and T. M. Yan, Phys. Rev. Lett. **25**, 316 (1970); Ann. Phys. (N.Y.) **66**, 578 (1971).

[13] J. C. Collins and D. E. Soper, Phys. Rev. D **16**, 2219 (1977); Nucl. Phys. **B193**, 381 (1981).

[14] C. Davies and W. J. Stirling, Nucl. Phys. **B244**, 337 (1984); C. Davies, B. Webber, and W. J. Stirling, *ibid.* **B256**, 413 (1985).

[15] NA10 Collaboration, S. Falciano *et al.*, Z. Phys. C **31**, 513 (1986); M. Guanziroli *et al.*, *ibid.* **37**, 545 (1988).

[16] E-615 Collaboration, J. S. Conway *et al.*, Phys. Rev. D **39**, 92 (1989); S. Palestini *et al.*, Phys. Rev. Lett. **55**, 2649 (1985).

[17] G. Marchesini and B. R. Webber, Nucl. Phys. **B330**, 261 (1990).

[18] M. Glück, J. F. Owens, and E. Reya, Phys. Rev. D **15**, 2324 (1978); B. L. Combridge, Nucl. Phys. **B151**, 429 (1979).

[19] P. Nason, S. Dawson, and K. Ellis, Nucl. Phys. **B303**, 607 (1988).

[20] At order α_s^3 the virtual corrections are also proportional to $\delta(q_\perp^2)$ and therefore do not contribute to the cross section at any finite $q_\perp^2 \neq 0$.

[21] R. K. Ellis and J. C. Sexton, Nucl. Phys. **B269**, 445 (1986); J. Gunion and Z. Kunszt, Phys. Lett. B **178**, 296 (1986).

[22] G. Altarelli, G. Parisi, and R. Petronzio, Phys. Lett. **76B**, 351 (1978).

[23] R. Kauffman, Phys. Rev. D **44**, 1415 (1991).

[24] I. Hinchliffe and S. F. Novaes, Phys. Rev. D **38**, 3475 (1988).

[25] S. Catani, E. D'Emilio, and L. Trentadue, Phys. Lett. B **211**, 335 (1988).

[26] Yu. L. Dokshitzer, D. I. Dyakonov, and S. I. Troyan, Phys. Rep. **58**, 269 (1980).

[27] A more detailed discussion on this point can be found, e.g., below Eq. (2.9) in Ref. [8] and in Ref. [26].

[28] G. Parisi and R. Petronzio, Nucl. Phys. **B154**, 427 (1979).

[29] J. C. Collins and D. E. Soper, Nucl. Phys. **B197**, 446 (1982); **B250**, 199 (1985).

[30] G. Altarelli, R. K. Ellis, M. Greco, and G. Martinelli, Nucl. Phys. **B246**, 12 (1984).

[31] P. B. Arnold and R. P. Kauffman, Nucl. Phys. **B349**, 381 (1991).

[32] C. P. Yuan, Phys. Lett. B **283**, 395 (1992).

[33] T. Han, R. Meng, and J. Ohnemus, Nucl. Phys. **B384**, 59 (1992).

[34] P. N. Harriman, A. D. Martin, W. J. Stirling, and R. G. Roberts, Phys. Rev. D **42**, 798 (1990).

[35] We have checked that the contribution to $d\sigma/dM^2$ from the processes (18), after a $q_\perp > 5$ GeV cut is applied, agrees with the shape of the lowest order result in the M^2 range shown in the figure.

[36] It has been pointed out by Catani *et al.* that matching does not always work; cf. S. Catani, L. Trentadue, G. Turnock, and B. R. Webber, Nucl. Phys. **B407**, 3 (1993).
[37] CDF Collaboration, F. Abe *et al.*, Phys. Rev. Lett. **64**, 142 (1990).
[38] G. Marchesini and B. R. Webber, Nucl. Phys. **B310**, 461 (1988).